

# Etching and morphology of poly(vinylidene fluoride)

A. S. VAUGHAN

*Polymer Science Centre, J. J. Thomson Physical Laboratory, University of Reading, Whiteknights, Reading RG6 2AF, UK*

The lamellar structures within spherulites of melt-crystallized poly(vinylidene fluoride) have been examined following the development of an etching technique which allows the study of representative morphologies in this polymer. The banded  $\alpha$ -spherulites, which predominate at crystallization temperatures below  $\sim 165^\circ\text{C}$ , are found to be made up of densely packed lamellae with an intrinsically planar habit, whilst the  $\gamma$ -spherulites which develop preferentially at higher temperatures, have a curious architecture in which the lamellae adopt a highly curved "scroll-like" morphology. These observations are discussed in terms of existing models for spherulite banding and non-planar lamellar habits.

## 1. Introduction

Much of the interest in poly(vinylidene fluoride) (PVF<sub>2</sub>) stems from its unusual piezoelectric and pyroelectric properties which may be induced by poling a particular crystal form in a strong electric field ( $\sim 1 \text{ MV cm}^{-1}$ ) [1-3]. Explanations of this behaviour have been proposed both in terms of trapped space charge [4, 5] and the reorientation of molecular dipoles within crystals and at lamellar surfaces [6-8]. Whilst the existence of carrier traps in PVF<sub>2</sub> has been demonstrated [9], as has the injection of metallic ions from the electrodes [10], there is also much strong evidence for the reorientation of crystalline dipoles. The evidence for dipolar reorientation arises from many sources, including X-ray investigations of structural changes during poling [6] and depolarization [11], and from the hysteresis-like curves of infrared transmittance that are obtained on varying the electric-field strength, the shapes of which have been successfully reproduced theoretically by Broadhurst and Davis [12]. Indeed, much theoretical work has been performed in an attempt to describe the polarization in PVF<sub>2</sub> in terms of a rotation of dipoles within crystallites in response to the imposed electric field [13-15]. However, a full evaluation of such theories, which attempt to include morphological information, requires the size and shape of the crystallites present in the material to be known.

Whereas such information may, in principle, be obtained by electron microscopy, the application of this technique to bulk-crystallized polymers is hindered by fundamental problems of sample preparation, intrinsically low contrast and severe radiation damage. Owing to the difficulty of preparing very thin sections of bulk-crystallized samples (i.e. less than 200 nm thick), most direct examination of polymers in the transmission electron microscope has been confined to simple solution-grown structures or to very

thin and, thereby, possibly unrepresentative films crystallized from the melt. As a consequence of the above problems, two less direct approaches have been developed for the examination of bulk-crystallized polymers. The first of these involves staining the sample, as in the chlorosulphonation of polyethylene [16], whilst in the second the surface of interest is first etched [17, 18] and then replicated, a shadowed carbon replica being examined in the electron microscope. This paper reports the first results obtained from the application of such an etching technique to PVF<sub>2</sub>. Although the etchant described does not contain manganese, the methodology has much in common with permanganic etching and, as such, may be considered as a further variant of this approach to the study of morphology in melt-crystallized polymers.

## 2. Experimental procedure

The samples examined in this work were crystallized from the PVF<sub>2</sub> resins Solef 1006 and Solef 1010 produced by Solvay et Cie, Brussels. Generally, samples were produced by melting a pellet of polymer between a slide and a cover slip on a Koffler hot bench, to produce a disc of material  $\sim 1 \text{ cm}$  diameter and  $\sim 200 \mu\text{m}$  thick. These samples were then placed in a Mettler hot stage and melted for 1 min at  $200^\circ\text{C}$  before being crystallized within the stage at the required temperature. Finally, the samples were quenched into cold water. Specimens prepared in this way will be referred to as thick films. Alternatively, some bulk samples were also produced by crystallization under an atmosphere of oxygen-free nitrogen in a silicone oil bath. Such samples were also  $\sim 1 \text{ cm}$  diameter but were several millimetres in thickness. In this case, internal surfaces for etching were prepared by microtoming.

In addition to its striking ferroelectric behaviour and good engineering properties, PVF<sub>2</sub> is also very resistant to chemical attack [19]; for this reason, PVF<sub>2</sub> is not amenable to normal permanganic etching. Therefore, a new etching technique was developed based on attack by fuming sulphuric acid, the precise reagent containing chromium trioxide and phosphorus pentoxide dissolved in solution in concentrated sulphuric acid. Experimentally, the etching reagent was made up as follows.

First, 10 g phosphorus pentoxide was added incrementally, with stirring, to 20 cm<sup>3</sup> concentrated sulphuric acid and left for ~30 min to dissolve. During this time ~60 mg chromium trioxide was accurately weighed out into a conical flask. When dissolution of the phosphorus pentoxide in the acid was complete, ~15 cm<sup>3</sup> of the solution was added to the chromium trioxide again with stirring, such that a 0.4% weight/volume solution was formed. After ~30 min, when the chromium trioxide had dissolved to give an orange solution, the etchant was ready for use. This reagent was then added to the PVF<sub>2</sub> samples and left for between 2 and 24 h at 90 °C, the exact time depending upon the samples under investigation and the relief required in the final etched surface. It was found, in addition to varying the etching time, to be necessary to modify the quantity of phosphorus pentoxide used, depending upon its water content and the amount of water present in the sulphuric acid. The best etching results were obtained from fresh reagents where neither the sulphuric acid nor the phosphorus pentoxide had been exposed to the atmosphere and where, as a result, the final etchant contained the lowest possible water content.

After the required etching time the samples were recovered as outlined below. First, the etchant was poured off into ~500 cm<sup>3</sup> water. This was performed with the utmost care because the reaction of the etching reagent with water is extremely violent. Once this had been completed the samples were washed twice in dilute sulphuric acid, then about six times in distilled water, with ~1 min between successive washes. Then the samples were washed twice in acetone, once for ~5 min in an ultrasonic tank. This last stage

was found to be important because, after etching, the samples were often covered in an orange/brown reaction by-product which prevented the formation of good replicas.

The surfaces etched as above were replicated using either a one- or a two-stage technique. For direct replication, the etched surfaces were shadowed with a platinum/palladium alloy and coated with carbon, the replica so produced being stripped from the polymer with poly(acrylic acid). This was then dissolved away by floating the polymer-backed carbon replica on distilled water. Finally, the clean replica was picked up from the surface of the water on an electron microscope grid, ready for examination. Alternatively, two-stage replicas were produced, in which an impression of the etched surface was first made in cellulose acetate, this being shadowed and carbonated as above. The acetate backing was then dissolved away in refluxing acetone to leave the replica on an electron microscope grid.

### 3. Results and discussion

The permanganic etching of polymers is a topic that has not been without controversy in some areas. In their original paper, Olley *et al.* [17] noted that under certain circumstances artefacts could be produced on the surface of etched polyethylene as a result, it was later found, of the precipitation of crystals from the etchant on to the sample [18]. Although with care, artefact formation was not a major limitation as far as the study of linear polyethylene was concerned, several workers did misinterpret artefacts as spherulites in, for example, investigations of morphology in cross-linked polyethylene cable insulations [20, 21]. Thus, in considering any proposed etching treatment it is of paramount importance to validate the technique as thoroughly as possible before indulging in any detailed interpretation of the images that result.

#### 3.1. Etching and PVF<sub>2</sub>

Fig. 1 shows two optical micrographs of PVF<sub>2</sub> crystallized at 160 °C. In (a), a surface treated with the

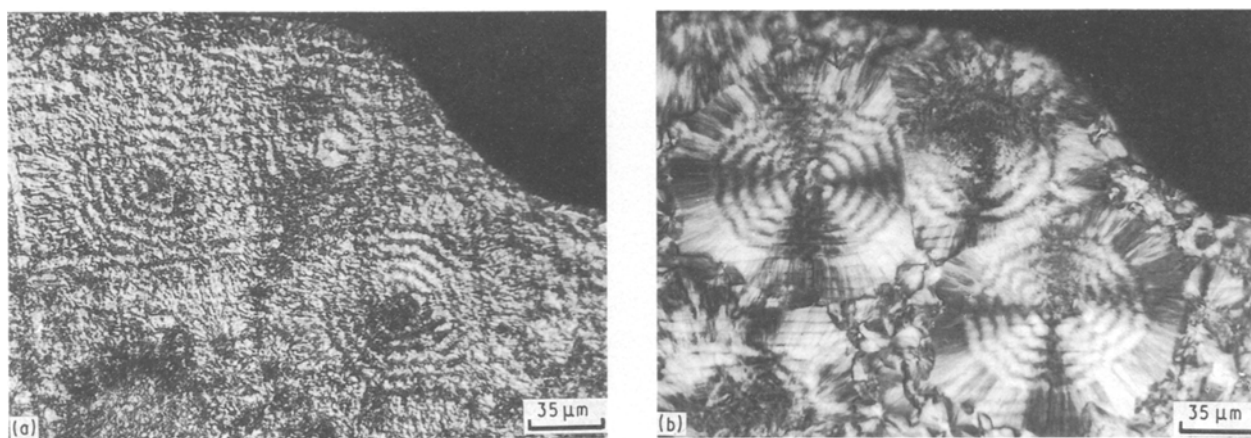


Figure 1 Optical micrographs of a sample of PVF<sub>2</sub> (Solef 1006) crystallized at 160 °C. (a) Etched microtomed surface as imaged using Nomarski differential interference contrast. (b) Transmission optical micrograph (polarized light) of a 5 μm thick section from adjacent to the etched surface shown in (a).

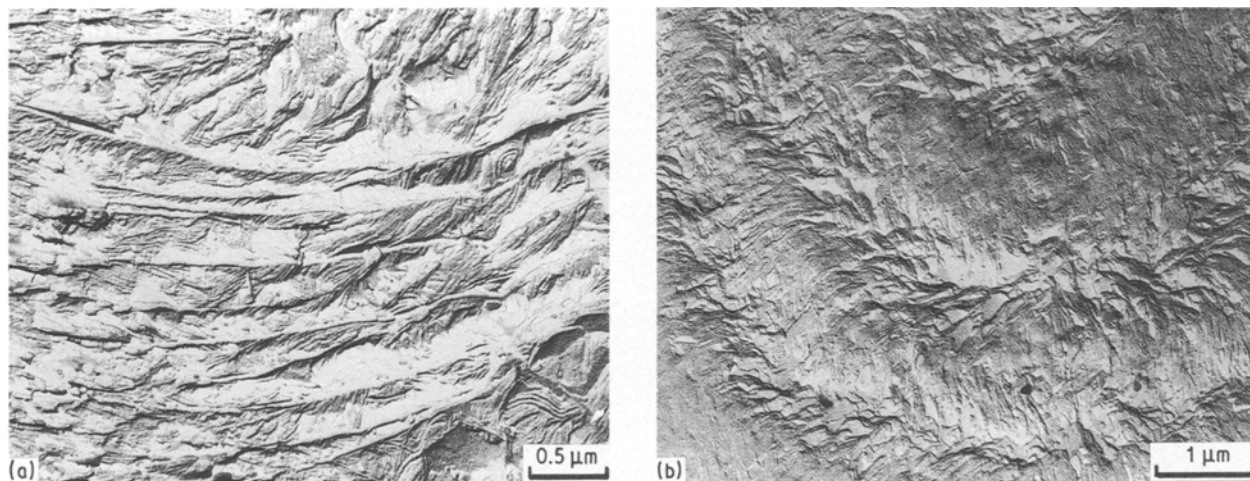


Figure 2 Microtomed samples of linear polyethylene following etching with the chromium trioxide-based reagent (two-stage replication). (a) Lamellar detail in a sample of HO 20 54P (BP Chemicals Ltd) crystallized isothermally at 128.4 °C. (b) Banded spherulitic structure in a quenched sample of R9 (BP Chemicals Ltd).

reagent described above is shown, imaged in reflection using Nomarski differential interference contrast, whilst in (b), a section removed from immediately above the etched surface can be seen viewed in transmission between crossed polars. Comparison of these two micrographs shows that where spherulite boundaries are seen in (b), corresponding features have also been revealed by etching in (a) and likewise, the banding which is clearly visible in (b) corresponds well with the bands seen in (a). Thus, at least at optical resolution, there is good reason to believe that the features revealed by etching are representative of the sample and are not merely artefacts of the chemical treatment. To further validate the etchant, samples of linear polyethylene were treated with the same reagent used to etch PVF<sub>2</sub>. Because both the new etchant described here and the conventional permanganic reagent rely upon oxidation by a transition metal complex in solution in sulphuric acid, it is reasonable to assume that the PVF<sub>2</sub> etchant should reveal structural features in polyethylene that are similar to those reported elsewhere [17, 18]. Fig. 2 shows micrographs of two samples of linear polyethylene. In both of these, lamellar detail is clearly evident, as is the banded nature of the spherulite shown in Fig. 2b. Indeed, the overall appearance is very similar to that seen in samples of linear polyethylene after treatment with the conventional permanganic reagent. Thus, on the basis of both optical and TEM evidence, it is clear that structural features revealed by the new etching reagent are genuine and are not merely artefacts arising from the etching process.

### 3.2. Banded spherulites of $\alpha$ -PVF<sub>2</sub>

Although PVF<sub>2</sub> is of practical concern because of its electro-active properties, its morphology is also of interest in its own right. PVF<sub>2</sub> may be processed to give a number of different crystal forms [22] ( $\alpha$ ,  $\beta$ ,  $\gamma$ , etc), and these may exhibit a wide range of different morphologies. However, isothermal crystallization from the melt at temperatures below  $\sim 165$  °C gen-

erally results in the formation of banded spherulites composed of lamellae of the  $\alpha$ -crystal form.

Fig. 3 shows two micrographs of a sample of Solef 1010 crystallized at 160 °C in the hot stage. The spherulite shown is composed of a dense mass of lamellae radiating from a centre and has a regularly banded structure typical of the  $\alpha$  crystal form of PVF<sub>2</sub> [23, 24]. Examination of the edge of this spherulite (Fig. 4) reveals a more open texture in which individual lamellae can be seen separated by regions of quenched melt. Thus, as in polyethylene [25–27], isotactic polystyrene [28] isotactic polypropylene [29], poly(ether-ether-ketone) [30], etc., spherulite growth occurs via an initial skeleton of individual dominant lamellae followed by later crystallization of subsidiary lamellae within the pre-established dominant framework. Such features are readily observed in samples such as that shown, which were crystallized in the form of a thin disc with a high surface area to volume ratio. In these samples, quenching occurs efficiently and little structure is observed between the isothermally crystallized spherulites. However, this is not the case when bulk samples several millimetres thick are prepared. In specimens of this type, mature spherulites may develop rapidly during quenching in regions where isothermal crystallization did not occur.

Such an object is shown in Fig. 5, revealed by etching an internal surface exposed by microtoming. This spherulite shows evidence of a central sheaf-like structure surrounded by radially grown lamellae, but with no banding. Although banded spherulites of  $\alpha$ -PVF<sub>2</sub> normally develop at low crystallization temperatures, investigations of quenching in PVF<sub>2</sub> have shown that, in addition to the glass,  $\alpha$ ,  $\beta$  and  $\gamma$  crystal forms may be produced, depending upon the quenching procedure used [31–33]. Thus, the spherulite shown in Fig. 5 may be composed of  $\gamma$  crystals or, alternatively, the absence of well-ordered bands may be attributable to the lamellae twisting in a non-cooperative manner.

Examination of the internal structure of banded  $\alpha$  spherulites of PVF<sub>2</sub> shows the variation of lamellar

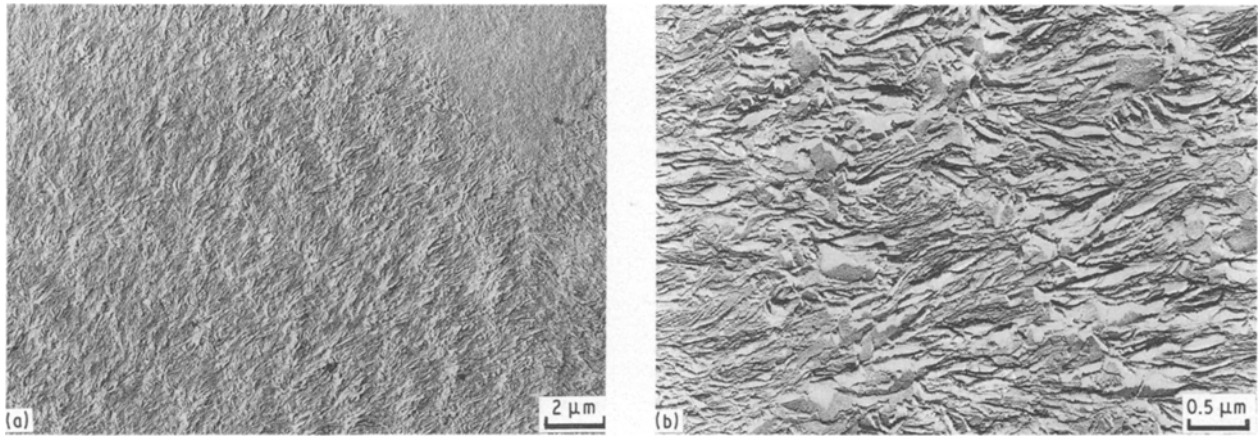


Figure 3 Etched thick film of PVF<sub>2</sub> (Solef 1010) crystallized at 160°C (two-stage replica). (a) Low-magnification micrograph showing the banded structure characteristic of  $\alpha$ -spherulites. (b) Detail showing the variation in lamellar orientation across the bands.

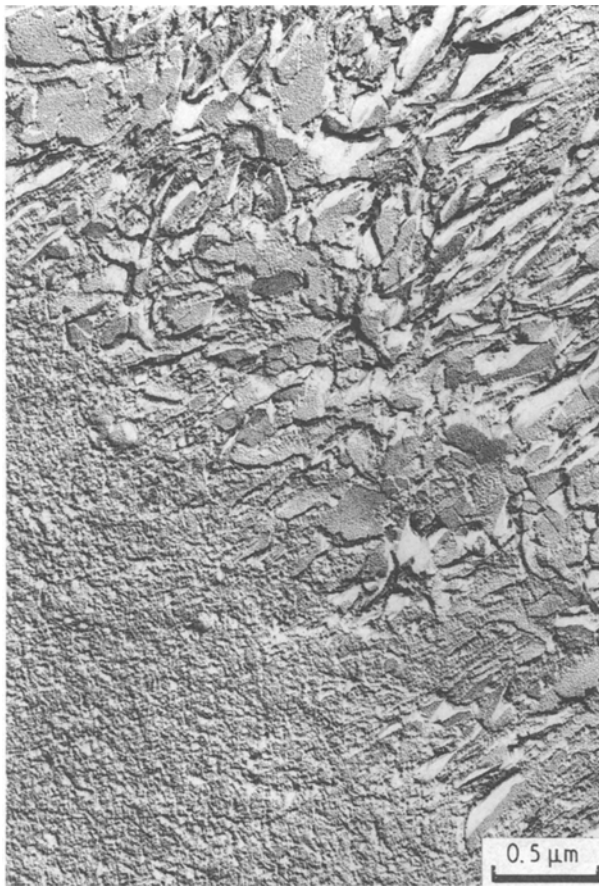


Figure 4 Edge structure of a spherulite grown isothermally at 160°C in a thick film of Solef 1010 and then quenched (two-stage replica).

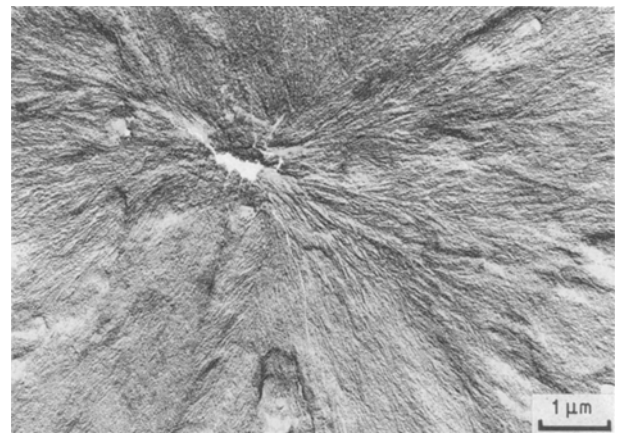


Figure 5 Etched microtomed surface of PVF<sub>2</sub> (Solef 1006; direct replica) showing a spherulite in a region of quenched melt.

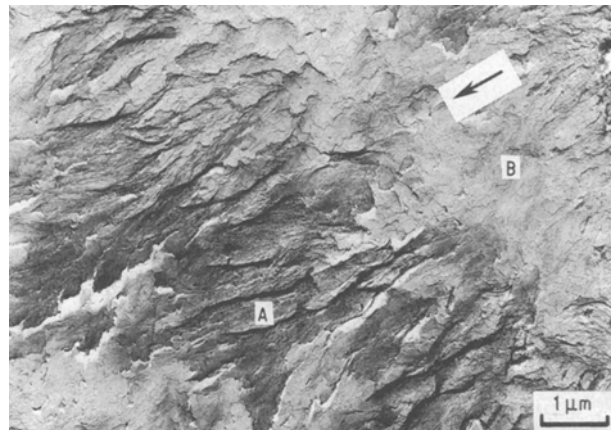


Figure 6 Etched thick film of PVF<sub>2</sub> (Solef 1006) crystallized at 163°C, two-stage replica. Variation of lamellar orientation within a spherulite of  $\alpha$ -PVF<sub>2</sub>. The radial crystallographic  $b$  direction is indicated by the arrow.

orientation which may be inferred from the optical microscope. Fig. 6 clearly shows this variation of average lamellar orientation about the spherulite radius, in which the direction shown here corresponds to the crystallographic  $b$  axis by electron diffraction, in agreement with previous work [19, 34]. At A, the lamellae are close to being viewed in the  $b \cdot c$  projection, i.e. edge-on, whilst at B the lamellae are viewed along the  $c$  axis, such that large areas of fold surface can be seen. From the examination of such regions, lamellae in  $\alpha$ -PVF<sub>2</sub> spherulites appear to develop with

a planar habit. Indeed, it has been reported that single crystals of  $\alpha$ -PVF<sub>2</sub> grown from dilute solution also grow as flat sheets [35]. However, early studies of the morphology of polyethylene [25–27] clearly demonstrated that the lamellar profiles present within a

spherulite are best determined when the structure is viewed along its radius; that is, lamellae are seen in the  $a \cdot c$  plane. Fig. 7 shows such a view, from which it can be concluded that the lamellae in melt-crystallized  $\alpha$ -PVF<sub>2</sub> do, indeed, have an intrinsically planar habit.

Conversely, in polyethylene, the only other system in which lamellar organization in banded spherulites has been studied in detail, the lamellae show curved cross-sectional profiles when viewed along their radial  $b$  direction and this has been systematically related to the presence of banding [27]. Keith and Padden [36] have further proposed that when lateral growth faces and fold surfaces are not orthogonal, as is the case in polyethylene, where the molecular chain stems are tilted with respect to the lamellar normals [37], different degrees of disorder may develop at opposite fold surfaces of one lamella and so set up stresses on opposing surfaces which are unequal. These disparate stresses then give rise to bending moments which result in the observed non-planar crystal habits and, when accompanied by asymmetrical development (as a result of diffusion processes or impingement), the formation of smoothly twisted helicoidal lamellae. However, no evidence was found in polyethylene for such uniformly twisted lamellae. Rather, what was reported were lamellae with little or no twisting for about one-third of a band period followed by a region in which more abrupt changes in orientation occurred [27]. This would also seem to be the case in PVF<sub>2</sub> (see Fig. 6). Nevertheless, Keith and Padden reconciled this apparent discrepancy by suggesting that the observed non-uniform twisting is not a feature of the initial dominant growth but rather results from subsequent subsidiary crystallization within the established interleaved dominant framework.

No evidence is as yet available concerning molecular canting within the lamellae that make up banded spherulites of  $\alpha$ -PVF<sub>2</sub>. However, in solution-grown crystals the molecular stems are reported to be perpendicular to the lamellar fold surface [19]. Thus, taking this indirect evidence, together with the cross-sectional profiles of lamellae shown in Fig. 7 and the apparently flat lamellae seen in certain regions of Fig. 6, it is difficult to reconcile the morphological

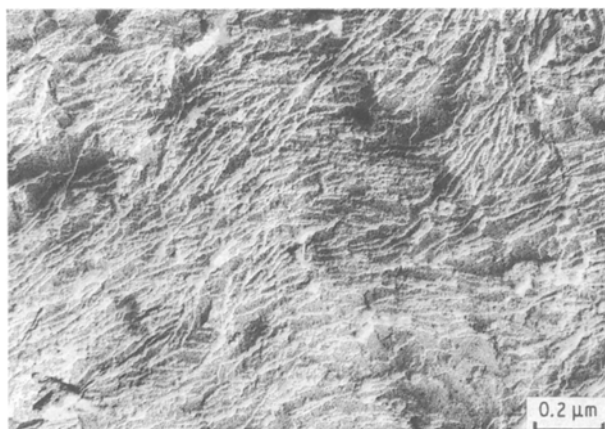


Figure 7 Etched thick film of PVF<sub>2</sub> (Solef 1006) crystallized at 163°C, two-stage replica. View down the radius of an  $\alpha$ -spherulite showing the intrinsically planar lamellar profile.

evidence with Keith and Padden's model for banded spherulites, as outlined above.

In view of the relatively discrete nature of lamellar reorientation in banded spherulites of both  $\alpha$ -PVF<sub>2</sub> and polyethylene, an alternative model for banding in polymeric spherulites that merits discussion is that due to Schultz and Kinloch [38]. This model considers the lamellar conformation in the vicinity of a screw dislocation, and the cumulative effect of a sequence of screw dislocations of the same hand. Many studies of both the melt [28] and solution [39] crystallization of polymers have clearly demonstrated that, during the growth of complex lamellar aggregates, such as spherulites and axialites, neighbouring lamellae tend to diverge. In addition, work in this laboratory has demonstrated that during the early stages of spherulitic growth of polyethylene, development occurs around isochiral giant screw dislocations [40]. Each screw dislocation is the same hand as those identified previously in individual melt-crystallized lamellae, being uniquely related to the sense of chain tilt within a lamella [41]. Around screw dislocations, lamellae diverge in such a way that each dislocation contributes an increment of radial twist. However, unlike polyethylene, there is no evidence for canted molecules in lamellae of  $\alpha$ -PVF<sub>2</sub> and, as a result, apparently no reason for screw dislocations of a particular hand to be preferred.

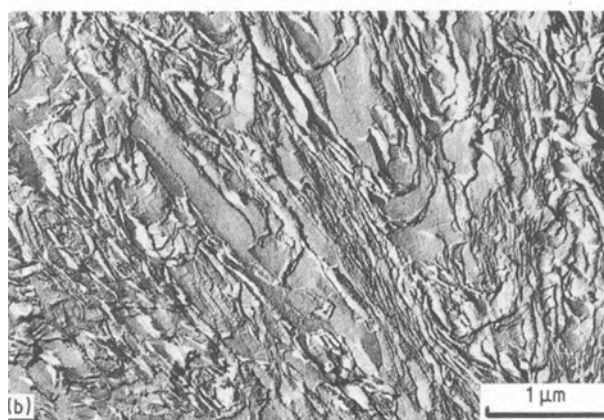
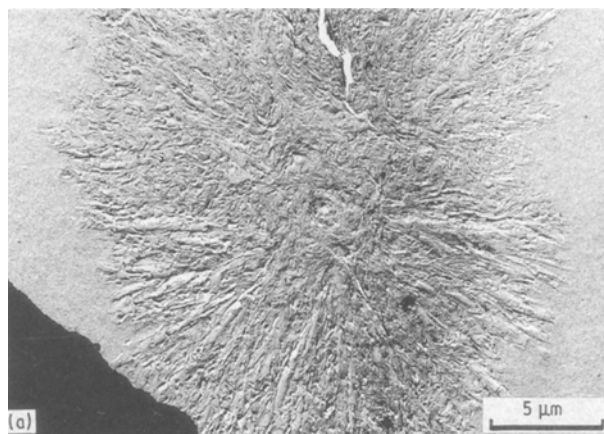


Figure 8 Etched thick film of PVF<sub>2</sub> (Solef 1010) crystallized at 172°C, two-stage replica. (a) Low-magnification view of a  $\gamma$  spherulite – no banding. (b) Detail showing radiating edge-on lamellae together with extensive areas of fold surface.



Figure 9 A spherulite of  $\gamma$ -PVF<sub>2</sub> (Solef 1010) grown at 172°C as seen when viewed down the radius. Thick film, two-stage replica.

### 3.3. Spherulites of $\gamma$ -PVF<sub>2</sub>

At this point it is appropriate to consider the other crystal form of PVF<sub>2</sub> that commonly develops during isothermal crystallization. Thin films of  $\gamma$ -PVF<sub>2</sub> crystallized from the melt on mica, give lamellae with a very regular habit in which the molecular chains are found to be inclined with respect to the lamellar normal (molecular inclination 28.5°) [42]. The above value is similar to that obtained for the chain inclination in polyethylene (~35°) [43] and in both systems the inclination occurs about the crystallographic *b* axis. In addition, it has been suggested that in mixed PVF<sub>2</sub> spherulites, the  $\gamma$ -unit cells are preferentially oriented with their *b* axes radial, i.e. in a similar orientation to that within polyethylene spherulites [37]. Thus according to the proposals outlined above, the lamellae in  $\gamma$ -PVF<sub>2</sub> spherulites would be expected to have a non-planar cross-sectional profile when viewed along the spherulite radius, and this should be accompanied by helicoidal twisting. Spherulites of  $\gamma$ -PVF<sub>2</sub> are, however, observed optically not to be banded [19].

Nevertheless, this does not eliminate the possibility of helicoidal lamellae, merely indicating the absence of cooperative twisting on the scale of optical resolutions. When such spherulites are examined in the electron microscope an unusual lamellar organization is revealed. Fig. 8a shows a spherulite of  $\gamma$ -PVF<sub>2</sub>. In this it appears that the lamellae possess a highly

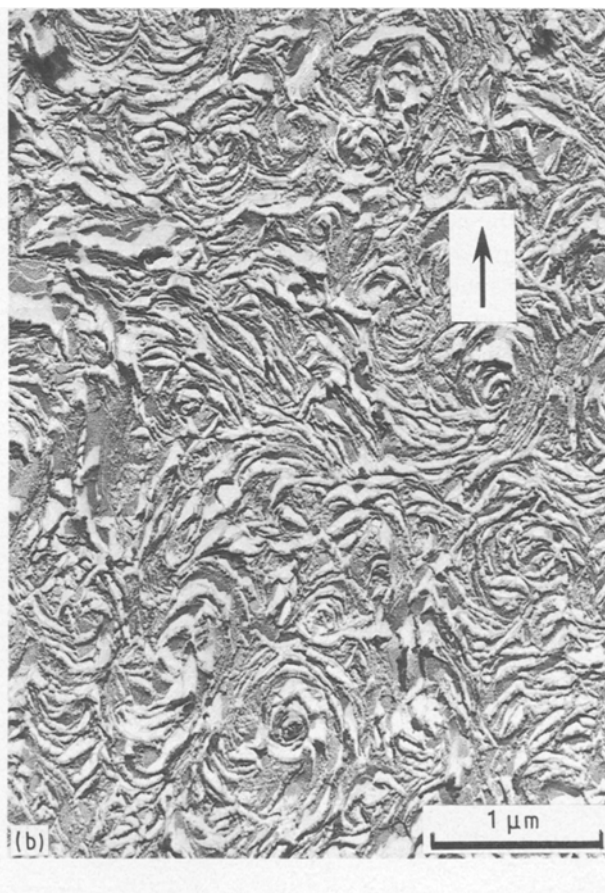
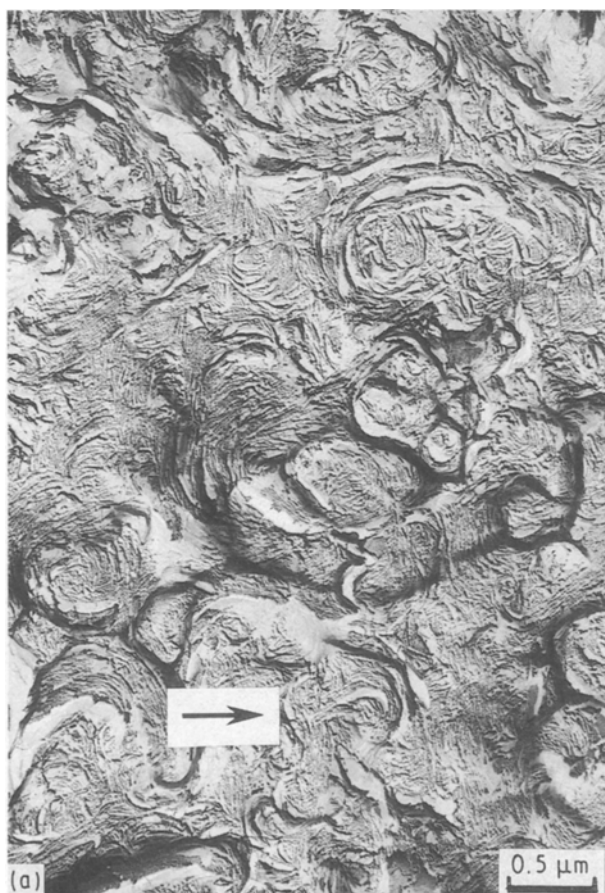


Figure 10 Lamellar profiles in  $\gamma$  spherulites viewed down their radial growth direction. (a) Etched cut surface in a sample of Solef 1006 crystallized at 168°C (direct replica). (b) Etched thick film of Solef 1010 crystallized at 172°C (two-stage replica).

elongated habit with no tendency whatsoever to twist about the radius, because in certain regions, where lamellae are viewed down the lamellar normal, long ribbon-like areas of the fold surface can be seen (see

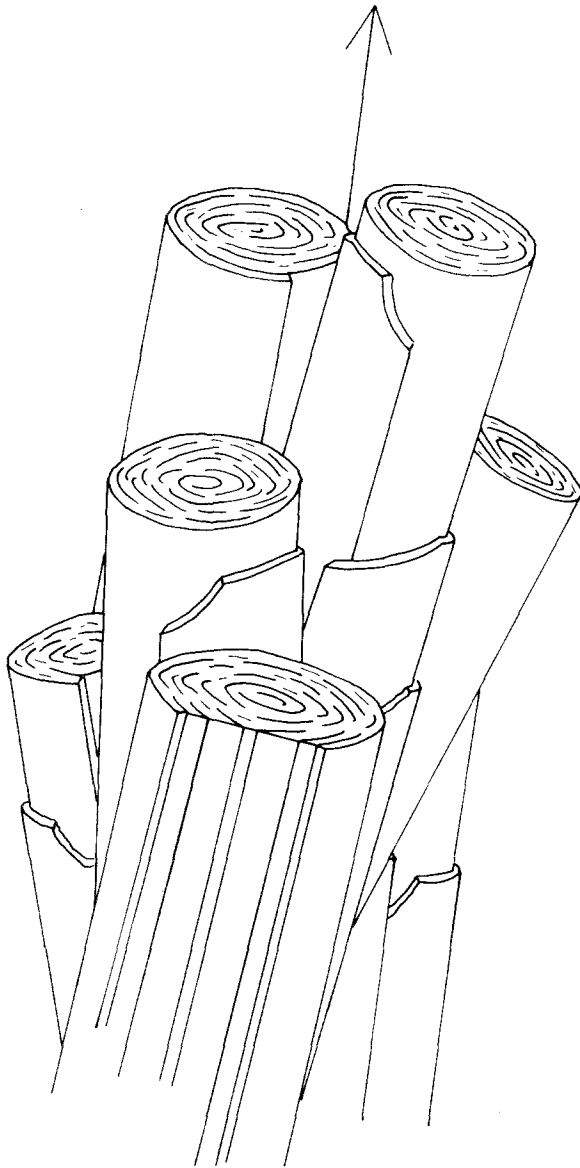


Figure 11 Schematic representation of the arrangement of lamellae in spherulites of  $\gamma$  PVF<sub>2</sub> showing the curved lamellar habit. The direction of the spherulite radius is as indicated by the arrow.

Fig. 8b). When such structures are viewed along the spherulite radius (see Figs 9 and 10), however, it can be seen that the lamellae exhibit a highly curved profile, similar to that previously reported for polybutene-1 crystallized from solution in amyl acetate [44]. Thus the spherulites' radial view is one of an arrangement of approximately circular cells, each filled with lamellae which are so highly curved as to present a scroll-like appearance (see Fig. 11). In addition, in Fig. 10, a few lamellae appear to have an S-shaped profile (examples are indicated by the arrow). However, due to the highly compact nature of this morphology, it is unclear whether such structures are genuine or merely appear due to the presence of two adjacent lamellae with opposite senses of curvature, such that a composite S-profile results.

From the above micrographs it can be seen that in  $\gamma$ -PVF<sub>2</sub> the inclination of molecular stems to the lamellar normal is, as in polyethylene, accompanied by curved profiles. Nevertheless, the model of Keith and Padden cannot account for the observed behaviour on grounds of symmetry. In addition, the extension of the model to account for banded spherulites does not appear correct in either  $\gamma$ -PVF<sub>2</sub>, where lamellar profiles are curved and spherulites are not banded, or in  $\alpha$ -PVF<sub>2</sub>, where banded spherulites are observed together with planar lamellae.

### 3.4. Poled PVF<sub>2</sub>

The results so far presented only consider samples of PVF<sub>2</sub> crystallized isothermally from the melt and then quenched. However, it is in connection with the piezoelectric and pyroelectric properties of this polymer that most technological interest lies. For this reason a sample of commercially produced piezoelectric PVF<sub>2</sub> sheet was examined using the novel etching technique previously described. Fig. 12a shows a micrograph of this material, in which a very fine-scale morphology can be seen. Although the individual constituent crystalline units are not ideally resolved, the structure appears to be one of an arrangement of small crystallites exhibiting a periodicity of  $\sim 30$  nm along the draw direction and with widths of the order of 200 nm.

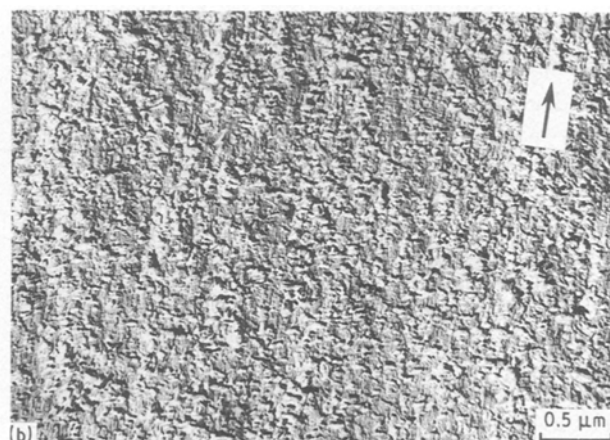


Figure 12 (a) Etched surface of a commercial sheet of poled PVF<sub>2</sub>, two-stage replica. (b) Etched surface of drawn polyethylene (courtesy Freedman [45]). In each case the arrow indicates the draw direction.

As may be expected, the observed structure is not unlike that seen in other drawn polymers. For comparison, a sample of drawn polyethylene (from [45]) is shown in Fig. 12b. Further interpretation of micrographs such as that of Fig. 12a is impossible at this stage, because details of the mechanical and electrical processing used in the manufacture of this commercial material are unknown. What is required, if an insight into the role of morphology in influencing the ferroelectric properties of PVF<sub>2</sub> is to be obtained, is a systematic examination of many samples subjected to various treatments ranging from simple melt crystallization, through various drawing and poling procedures, finally, to both mechanical and electrical processing. Then, using the TEM technique described, the observed morphological features may be understood in terms of those initially present in the material together with the effect of the various processing stages.

#### 4. Conclusion

From this initial study of the morphology of PVF<sub>2</sub> it can be concluded that crystallization from the melt leads to well-ordered spherulites which grow by the same dominant/subsidiary mechanism previously identified in other systems. In the banded spherulites of the  $\alpha$ -crystal form, the radial growth direction is *b* and the lamellae adopt a planar habit. Solution crystallization also gives planar lamellae, which are pseudo-hexagonal and extended along the crystallographic [0 1 0] direction, with the molecular chain axis perpendicular to the plane of the lamellae. The similarities between the melt and solution cases suggests that the molecules may also be parallel to the lamellar normals in  $\alpha$  lamellae crystallized from the melt. In the  $\gamma$  crystal form of PVF<sub>2</sub>, however, the molecules are known to adopt an inclined conformation with respect to the lamellar normal, and in  $\gamma$  spherulites, which are not banded, lamellae are seen to exhibit a non-planar habit. These observations are only partly in agreement with proposals that canted molecular configurations give rise to non-planar lamellar habits. Specifically, the results presented here for PVF<sub>2</sub> do not concur with the extension of such ideas as a general explanation for banding in spherulites. In addition, at this time, there is no apparent reason for left- and right-handed screw dislocations to be energetically non-degenerate in PVF<sub>2</sub>, as is required for the screw-dislocation-based models for banding, and thus at present these ideas also appear unable to account satisfactorily for the structures seen in  $\alpha$ -PVF<sub>2</sub>.

#### Acknowledgements

The author thanks Dr A.M. Freedman for providing Fig. 12b and Professor D.C. Bassett for his helpful suggestions and comments concerning the work described.

#### References

1. J. I. SCHEINBEIM, C. H. YOON, K. D. PAE and B. A. NEWMAN, *J. Polym. Sci. Polym. Phys. Ed.* **18** (1980) 2271.
2. H. VON SEGGERN and T. T. WANG, *J. Appl. Phys.* **56** (1984) 2448.
3. M. LATOUR and R. L. MOREIRA, *Ferroelectrics* **76** (1987) 427.
4. N. MURAYAMA and H. HASHIZUME, *J. Polym. Sci. Polym. Phys. Ed.* **14** (1976) 989.
5. K. TAKAHASHI, H. LEE, R. E. SALOMON and M. M. LABES, *J. Appl. Phys.* **48** (1977) 4694.
6. R. G. KEPLER and R. A. ANDERSON, *ibid.* **49** (1978) 1232.
7. G. T. DAVIS, J. E. MCKINNEY, M. G. BROADHURST and S. C. ROTH, *ibid.* **49** (1978) 4998.
8. E. FUKADA, M. DATE, H. E. NEUMANN and J. H. WENDORFF, *ibid.* **63** (1988) 1701.
9. Y. SUZUOKI, T. MIZUTANI, M. SHIMOZATO, N. SUGIURA and M. IEDA, *Jpn. J. Appl. Phys.* **19** (1980) 861.
10. S. OSAKI and Y. ISHIDA, *J. Polym. Sci. Polym. Phys. Ed.* **11** (1973) 801.
11. A. J. BUR, J. D. BARNES and K. J. WAHLSTRAND, *J. Appl. Phys.* **59** (1986) 2345.
12. M. G. BROADHURST and G. T. DAVIS, Annual Report, Conference of Electrical Insulators and Dielectric Phenomena (IEEE, New York, 1979) p. 447.
13. M. G. BROADHURST, G. T. DAVIS, J. E. MCKINNEY and R. E. COLLINS, *J. Appl. Phys.* **49** (1978) 4992.
14. K. TASHIRO, M. KOBAYASHI, H. TADOKORO and E. FUKADA, *Macromolecules* **13** (1980) 691.
15. J. GANSTER and D. GEISS, *Polymer* **26** (1985) 1825.
16. G. KANIG, *Z. Z. Koll. Polym.* **251** (1973) 782.
17. R. H. OLLEY, A. M. HODGE and D. C. BASSETT, *J. Polym. Sci. Polym. Phys. Ed.* **17** (1979) 627.
18. R. H. OLLEY and D. C. BASSETT, *Polymer* **23** (1982) 1707.
19. A. J. LOVINGER, in "Developments in Crystalline Polymers-1", edited by D. C. Bassett (Applied Science, London, 1982) p. 195.
20. J. MACCIGROSSO and P. J. PHILLIPS, *IEEE Trans. Electr. Insul.* **EI-13** (1978) 172.
21. L. A. DISSADO, J. C. FOTHERGILL and S. V. WOLFE, Annual Report, Conference on Electrical Insulators and Dielectric Phenomena, (IEEE, New York, 1981) p. 264.
22. N. A. SUTTLE, *GEC J. Res.* **5** (1987) 141.
23. A. J. LOVINGER, *J. Polym. Sci. Polym. Phys. Ed.* **18** (1980) 793.
24. B. S. MORRA and R. S. STEIN, *ibid.* **20** (1982) 2261.
25. D. C. BASSETT and A. M. HODGE, *Proc. R. Soc. Lond.* **A377** (1981) 25.
26. D. C. BASSETT, A. M. HODGE and R. H. OLLEY, *ibid.* **A377** (1981) 39.
27. D. C. BASSETT and A. M. HODGE, *ibid.* **A377** (1981) 61.
28. D. C. BASSETT and A. S. VAUGHAN, *Polymer* **26** (1985) 717.
29. D. C. BASSETT and R. H. OLLEY, *ibid.* **25** (1984) 935.
30. D. C. BASSETT, R. H. OLLEY and I. A. M. AL RAHEIL, *ibid.* **29** (1988) 1745.
31. C. C. HSU and P. H. GEIL, *J. Appl. Phys.* **56** (1984) 2404.
32. *Idem*, *Polym. Commun.* **27** (1986) 105.
33. D. YANG and Y. CHEN, *J. Mater. Sci. Lett.* **6** (1987) 599.
34. A. J. LOVINGER and T. T. WANG, *Polymer* **20** (1979) 725.
35. D. T. GRUBB and K. W. CHOI, *J. Appl. Phys.* **52** (1981) 5908.
36. H. D. KEITH and F. J. PADDEN, *Polymer* **25** (1984) 28.
37. D. C. BASSETT, "Principles of Polymer Morphology" (Cambridge University Press, Cambridge, 1981).
38. J. M. SCHULTZ and D. R. KINLOCH, *Polymer* **10** (1969) 271.
39. D. C. BASSETT, A. KELLER and S. MITSUHASHI, *J. Polym. Sci. A 1* (1963) 763.
40. M. SHAHIN, PhD thesis, Mansoura University (1989).
41. D. C. BASSETT, R. H. OLLEY and I. A. M. AL RAHEIL, *Polymer* **29** (1988) 1539.

42. A. J. LOVINGER and H. D. KEITH, *Macromolecules* **12** (1979) 919.
43. J.-J. LABAIG, PhD thesis, L' Université Louis Pasteur de Strasbourg (1978).
44. V. F. HOLLAND and R. L. MILLER, *J. Appl. Phys.* **35** (1964) 3241.
45. A. M. FREEDMAN, PhD thesis, University of Reading (1987).

*Received 15 October 1991  
and accepted 14 August 1992*